COHERENT NOISE FILTERING USING RECONSTRUCTED PHASE SPACE

Jesus Silva Castro, Kleydis Suarez, Dominique Jeantet, Christian Germain

COHERENT NOISE FILTERING USING RECONSTRUCTED PHASE SPACE

Jesus Silva-Castro[(a)], Kleydis Suárez[(a,b)], Dominique Jeantet[(a)], Christian Germain[(a,d)].

[(a)] Laboratoire de l'Intégration du Matériau au Système(IMS), UMR 5218, CNRS, Bordeaux University, BP. 99, F-33402, Talence - Cedex, France.

[(b)] Universidad Simón Bolívar. Sartenejas, Baruta, Edo. Miranda – Apto. 8900. Venezuela

[(c)] Ecole Nationale Supérieure d'Electronique Informatique & Radiocommunication de Bordeaux (ENSEIRB), Av. Dr A. Schweitzer, BP 99, F-33402, Talence - Cedex, France.

[(d)] Ecole Nationale d'Ingénieurs des Travaux Agricoles de Bordeaux (ENITAB), 1 cours du Général de Gaulle, CS 40201, F-33175, Gradignan - Cedex, France.

Corresponding author*:*

Telephone number: +33 5 40 00 24 00.

Fax number: +33 5 40 00 66 44.

E-mail address: Christian.germain@ims-bordeaux.fr

Abstract

Within the framework of coherent noise attenuation, this paper describes an original filtering approach based on the dynamical system theory. The reconstructed phase space is used to interpret dynamical behavior of image measurements, i.e. of local pixel amplitudes. Originaly developed for time series, the method of delays allows reconstructing steady-state trajectories from measurements of a physical system. This contribution suggests a method of delays adapted to the 2D data issue. The phase space of an image is defined as vectors-axes in a Cartesian plane, containing the pixel amplitude at spatially delayed coordinates, the latter selected according to a directional neighborhood criterion. The space proposed helps to evaluate the statistical properties of local structures within the image. Structures with similar local dynamics occupy nearby locations in phase space. These dynamical properties allow modelling local periodic patterns corrupting the image, such as the coherent noise. The Average Phase Space (APS) is a modified frequency distribution map that consists of the amplitude mean of trajectories points. For the proposed filter, each pixel value of the output image corresponds directly to the APS magnitude at the location associated with the original pixel image. APS method is applied to synthetic and real noisy images. Findings indicate that APS filtering is a low-cost algorithm for coherent noise attenuation that preserves the quality of edges in images.

Keywords: Coherent noise, dynamic behavior, image processing, nonlinear filters, phase space,

1. Introduction

One of the most complex challenges in image processing is noise attenuation, while preserving underlying data features. Noise appears as a result of various physical processes which impair the image quality. Unfortunately, such noise diversity demands the use of specialized processing approaches. Image processing methods, used in particular on seismic, tomographic, optical and radar data, resort to statistical tools to attenuate coherent noise.

Coherent noise (CN) is a structured noise observed in an image as repetitive and periodic patterns and it is a common problem in applications associated with the use of switching power supplies, which are on-board detection devices. Sinusoidal CN components and harmonics are observed scattered throughout the frequency spectrum. Indeed, a Discrete Fourier Transform (DFT) analysis would show frequency, phase, and magnitude of CN components varying over time [1]. Given its nature, CN cannot be effectively attenuated by simple averaging techniques.

CN attenuation is a critical step in several applications. One straightforward method for reducing coherent noise is a band-pass filter applied to radial traces [2]. Radial trace concept comes from 3-D geophysics data analysis and depicts the use of vertical series of voxels as 1-D signals. Radial Trace Transform operates over the juxtaposed traces and the stacked sections of 3D-data, transforming the familiar horizontal distance and the travel time (X-T) domain into the domain of apparent velocity and travel time [3][4]. Other approaches introduce filtering methods based on Prediction Error Filters (PEF), estimated either by approximating an inverse covariance matrix or by modeling the coherent noise. Both strategies are based on the spectral whitening properties of PEFs. The first strategy makes use of the fundamentals of inverse theory [5][6]; whereas the second consists of modeling CN by diagonal operators, estimated using least-squares methods [7]. Gockenbach and Symes [8] proposed a filtering approach to coherent noise rejection based on velocity analysis, formulated as an inverse problem. More recently, Guitton [9] obtained excellent results in the distance-time domain by implementing non-stationary PEFs to cope with the variability of seismic data as a function of time, offset, and shot position. Nevertheless, residual coherent noise remains in his findings. Another approach that makes use of velocity analysis is the f-k transformation [10], a common method for separating seismic reflections from noise by a 2D Fourier transformation. The x-axis is transformed to the wavenumber domain. The number of wavelengths per meter along the horizontal axis indicates the wavenumbers, k. Therefore, the slope of

a line in f-k domain is the apparent velocity, v_a, since the relation between the frequency domain and the wavenumber domain is $f = v_a k$. More general filters, such as the orientation adaptive (OA) Gaussian filters introduced by Bakker [11], exploit spatial redundancy in images. The OA Gaussian approach uses the Gradient Structure Tensor (GST) to estimate orientation, gradient energy and anisotropy [12]. Nonetheless, this method depends on the quality of orientation estimations and it tends to produce false structures ("brushstrokes"). To cope with this weakness, O'Malley and Kakadiaris [13] proposed the orientation-isotropy adaptive (OIA) Gaussian filter, which considers the well-oriented texture of an image in order to take advantage of OA Gaussian properties.

In this paper, we propose a new approach to characterize and to reduce coherent noise, using a dynamical representation known as phase space [14]. Initially introduced by Poincaré [15], phase space provides a geometric approach for analyzing qualitatively the global state from insoluble differential equations of dynamical systems. In the original version, phase space represents a Cartesian plane where the principal state-variables, such as a body's position and momentum (velocity), form the coordinate axes. Poincaré established a general classification of solutions in two-dimensional phase space in terms of singular points, such as centers, saddle points, nodes, and foci. His major finding was that among all the curves not ending in a singular point, some are periodic (they are limit-cycles): all others wrap themselves asymptotically around limit-cycles. Every curve in this space denotes a trajectory, i.e. an evolution-state of the dynamical systems. Phase Space (PS) has been a useful tool in mathematics and physics for visualizing the changes in the dynamics of a system. Applications of phase space representations extend to hydrodynamics, the stability of laminar flows [16] , turbulence analysis [17], automatic control and regulation [18]. The study of stabilization of oscillatory phenomena, resonance, and feedback loops by phase space has also played an important role [19], in particular for cybernetics.

Takens [17], Packard [20] and Sauer [21] proposed a reconstruction theorem based on the *embedding dimension*. This leads to obtaining the phase space of those systems for which their state equations are not available. Hence, the reconstruction theorem has made it possible to analyze the dynamic information of processes described by temporal signals. The most frequently used reconstruction technique for time series is the Method Of Delays [22], which uses instantaneous and differential values of a signal to define the coordinate axes in the new phase space.

In this paper, we suggest characterizing the dynamic behavior of CN in images by a reconstructed phase space approach. In section 2, an original method is introduced, based on the embedding theory to solve the reconstruction problem of phase space from 1D to 2D data. Section 3 presents the statistical measures proposed to emphasize periodic and repetitive patterns in the phase space reconstructed from noise-corrupted images. Section 4 describes the image filtering method based the phase space. A comparative analysis in section 5 illustrates the performance of our approach when applied to synthetic and tomographic images. Finally, a summary relating main aspects of this contribution is available in section 5.

2. The Reconstructed Phase Space from an Image

Most of the specialized work on the reconstruction theorem has been defined exclusively for 1D data [22]. This is the case for temporal series $x_k = x(kT_S)$ in Euclidean space R^m, for the $k = 1,\ldots,N$ samples and T_s the sampling time. In this section, the reconstruction of phase space from data with multidimensional information, e.g. image data is performed. Dynamical information in 1D-signals is obtained from magnitude and time values. In images, however, the dynamic information also involves properties such as local amplitude and spatial coordinates of pixels. Moreover, image information depends not only on multi-spectral properties, but also on local context, defined by the pixel neighborhood. Therefore this work considers a reconstructed phase space that associates amplitude value and the definition of neighborhood of image pixels.

Literature shows that one-dimensional time series can be unfolded into an *m*-dimensional phase space. According to Takens theorem [17], if the number *m* denoting the dimension of reconstructed phase space is large enough, the phase space is homeomorphic to the state-space that generated the time series, i.e. the phase space contains the same information as the original state space. Given a time series, x_k, the Method of Delays used to reconstruct the phase space considers *m*- vector axes containing the time delayed values of the signal scalar measurements [14]:

$$X_k^m = \left[x_k, x_{k+\alpha}, \ldots, x_{k+(m-1)\alpha}\right]^T \quad (1)$$

where α is a time delay or gap and *m* is the embedding dimension. For this reason, the reconstructed phase space is also known as embedding space. The definition of time lag and embedding dimension that

ensure proper reconstruction is an open problem in dynamics analysis. The embedding dimension requires a priori knowledge about experimental data that is not often available. A common algorithm used to estimate *m* dimension is based on the false nearest neighbors approach [24]. On the contrary, Holzfuss and Mayer-Kress [25] proposed an approach based on mutual information to choose the α -factor. The first local minimum in the autocorrelation function determines a well-adapted α time delay value.

By analogy, we propose to reconstruct the phase space associated with image matrix ***I***(*N*,*M*), as an Euclidean space R^m defined by the *m*-dimensional reconstructed state vectors:

$$G_{i,j}^{m} = [I(i,j), I((i,j)+\beta), \ldots, I((i,j)+(m-1)\beta)] \tag{2}$$

where *I*(*i*,*j*) is the amplitude of a pixel at the (*i*,*j*)-spatial coordinate, and β is a spatial-delay factor along a chosen direction in the image. The Cartesian coordinate system in the proposed phase space yields vector-axes that contain the amplitude of such pixels selected according to a precise directional choice. We choose a two dimensional phase space, *m=2*, to depict the dynamic behavior of images. We further consider a 4-neighborhood to describe the β -factor, i.e. pixels above, below, to the left and to the right of the central pixel correspond respectively to $\beta = \{(0,-\alpha);(0,\alpha);(-\alpha,0);(\alpha,0)\}$. The scalar value α indicates the coordinate gap of the spatial-delay. Figure 1 illustrates the 4-neighbour local information of a pixel with local amplitude '*g*', located at the *(i,j)*-spatial coordinate in the image ***I***(*M*,*N*). We denote "locus" the location of points in the phase space. A pixel intensity at the (*i*,*j*)-coordinate in the original image data has a projection at [*k*,*l*]-locus in the reconstructed phase space.

Figure 2 presents a synthetic image and its reconstructed phase space. In this case, abscissa and ordinate are the amplitude vectors of pixels ***I***(*i*,*j*) and ***I***(*i*,*j+1*) respectively. They denote the vectors (eq. 2) established using a mono-directional choice, i.e. one spatial-delay vector $\beta = (0,\alpha)$ with $\alpha = 1$. Locus notation in this figure is [*k*,*l*]=[***I***(*i*,*j*), ***I***(*i*,*j+1*)]=[*g*, g_S]. Note that the phase space in figure 2*b* shows a limit-cycle trajectory associated with the vertical periodic component in the image. However, harmonic components added to this image generate trajectories with embedded loops (figure 3), which depict quasi-periodic limit sets [23].

2.1. Directional choice

Directional choice depends on the orientation of the phenomenon to be analyzed in the image. As illustrated in figures 2 and 3, mono-directional choice helps to study respectively horizontal and vertical

image patterns. However, more complex patterns require considering multi-directional neighborhoods. We propose an arithmetic mean operator to define 2-neighbors connectivity for each phase space axis. For instance, we define a [*k,l*]-locus combining 4-neighborhoods:

$$k = \frac{g_S + g_E}{2}, \quad l = \frac{g_N + g_W}{2} \tag{3}$$

Figure 4 shows a grey-level image with repetitive patterns and the corresponding phase spaces estimated using two distinct directional neighbor configurations. In these images, we observe that each neighbor configuration characterizes a particular viewpoint of the same dynamical phenomenon (fig. 4b and 4c).

For 3D images, the directional choice must incorporate the additional dimension, i.e. upper and lower voxels, g_U and g_D respectively. Figure 5 shows the neighborhood of a voxel. We suggest projecting the 3D information into a locus according to this criterion:

$$k = \frac{g_S + g_E + g_D}{2}, \quad l = \frac{g_N + g_W + g_U}{2} \tag{4}$$

In the case of a 3D phase space (m = 3), the choice of coordinate vectors [*k,l,h*] becomes:

$$k = \frac{g_W + g_E}{2}, \quad l = \frac{g_N + g_S}{2}, \quad h = \frac{g_U + g_D}{2}, \tag{5}$$

3. The Coherent Noise characterization in the reconstructed phase space

In the phase space, data with local periodic behaviors shows trajectories such as limit-cycles and embedding loops. Structures with similar local information occupy nearby loci in phase space. As a result, coherent information will clearly show groups of points following a geometric structure in the phase space. Figure 6 illustrates the phase space for Gaussian and coherent noises. Note that periodic and repetitive characteristics of coherent noise delineate trajectories (figure 6*d*), which are quasi-periodic limit sets, in the phase space. Conversely, the Gaussian noise shows scattering in phase space (figure 6*c*).

The frequency distribution of each local structure is considered as measuring the repetitiveness of the coherent noise. We define $f_{L(k,l)}$ as the cumulative (statistical) frequency relative to locus $L(k,l)$, i.e. the number of pixels in the original image projected on the same locus in the phase space. Figure 7 is a 3D

histogram that displays the repetitiveness $f_{L(k,l)}$, associated with pixels projected to each locus $L(k,l)$ of the figure 4*a*.

4. Filtering Method: The Average Phase Space

4.1. Data

We develop 2D techniques analogous to classical image processing, such as the averaging operator, based on phase space representation. The statistical locus information from phase space is used to design a nonlinear average filter. We exercise the proposed method on synthetic and real images.

Figure 8*a* illustrates a synthetic textured image which includes a fault line. Moreover, the bottom-right corner of this image is corrupted using a repetitive pattern. In this test, the goal of the filtering method is to reduce the noise while preserving the sharpness of the artificial "fault line".

Figure 9 results from the section of a 3D tomographic block. It shows structures of a fiber-reinforced composite material. A reconstruction artifact shaped as concentric circles, as well as various noise sources, corrupt the block. For this type of exercise, the goal is to attenuate coherent noise, while preserving the quality of object boundaries inside the material.

4.2. Method

The proposed method operates in two stages: noise characterization and filtering. In the first step, the phase space of image $\boldsymbol{I}$ is reconstructed using the pixel intensity vectors of a pre-selected neighborhood. The orientation of artifact to be filtered is considered in order to establish the directional neighborhood. Thereafter the frequency distribution map, f_L is computed as explained in section 2. Furthermore, the Average Phase Space (APS) is defined as a modified frequency distribution map that includes the amplitude mean of each locus $L(k,l)$. That is:

$$APS_{L(k,l)} = \frac{\sum_{L(k,l)} I(i,j)}{f_{L(k,l)}} \tag{6}$$

Note that locus $L(k,j)$ is computed using the neighbors of pixel $\boldsymbol{I}(i,j)$ according to directional considerations (eq. 3). Figure 10 shows the APS calculated from the image in figure 4*a*. The final stage

uses the APS to produce the filtered output image. Each pixel value of the output image directly corresponds to the APS magnitude at the locus associated with original pixel image { (*i,j*) ➔ [*k,l*] }.

$$I_{OUT}(i,j) = APS_{L(k,l)} \tag{7}$$

where $I_{OUT}(i,j)$ is the filtered (i,j)-pixel value. Finally, the APS results are compared with those of the OIA filter [13].

5. Results and Discussion

5.1. Synthetic data

In figure 11, APS approach is applied to a synthetic coherent noised-contaminated image. Figures 11*a* and 11*b* respectively show the original image and its phase space. The corrupted image and its phase space are presented in figures 11*c* and 11*d*. The APS filtering is illustrated in figures 11*e* and 11*f*. It should be observed that the APS filter preserves zones associated with loci with low statistical frequency, such as in the vicinity of the fault line.

5.2. Textured image

With the careful choice of the neighborhood, the APS filter can be used as a directional filter. For instance in figure 12*a*, the horizontal line patterns of the Brodatz texture image D51 [26] are observed. The APS filter estimated from this image considers two mono-directional neighborhood choices, either exclusively horizontal (Fig. 12*b*) or exclusively vertical (Fig. 12*c*). In figure b, the APS filter preserves the horizontal lines, whereas in (Fig. 12*e*). the horizontal lines have been smoothed.

5.2. Tomographic data

The low computing cost of the APS filters makes it particularly worthwhile for 3D data processing. Image in figure 13*b* was obtained using an OIA Gaussian filter on a 200×200×198 tomographic block (figure 13*a*). Figure 13*c* shows the image filtered by the APS method using 3D information and a 3D phase space (eq. 5). Both filters attenuate coherent noise although the OIA Gaussian method introduces artifacts (see zooming in figures 14*b* and 14*c*). For this block, the OIA filter takes, on average, 30 minutes, compared to 30 seconds taken by APS filtering after two iterations.

5. Summary

The dynamical systems theory, widely used in numerous 1D applications, was extended in this work to the image processing field. Taken's theorem was adapted to the problem of the phase space reconstruction from 1D to 2D data, by a spatial-delay mapping approach. Phase space shows geometrical trajectories associated with the image dynamics, grouping periodic structures such as coherent noise into ordered regions. Hence, similar patterns can be observed in nearby loci. Phase space provides valuable information for filtering purposes. Coherent-noise features, such as the repetitiveness, including statistical characteristics can be characterized in the reconstructed phase space. A frequency distribution map was used here to design a nonlinear average image filter. The APS filter presents a very low computing cost, which proves to be well-adapted for processing large data. The APS methods combine neighborhood analysis and statistical processing in images; consequently the overall performance of this method grows with the size of data samples analyzed in the phase space.

Future improvements to this approach will consider studies about efficiency of the algorithm as a function of image size, the tuning of the parameters (m and α values), and automatic neighborhood determination. Generally, the proposed image processing technique should be worthwhile for the study of chaotic phenomena in 2D and 3D data.

Acknowledgement

We thank P. Baylou, Y. Berthoumieu and L. Valente for their valuable comments and suggestions. The authors would also like to thank Prof. G. L. Vignoles, O. Coindreau (LCTS), SPS-SAFRAN and the ESRF (European Synchrotron Radiation Facility) ID 19 team for providing us with the composite material 3D data.

References

[1] R. Bracewell, The Fourier Transform and Its Applications. McGraw-Hill, USA, 1965.

[2] D.C. Henley, The radial trace transform: an effective domain for coherent noise attenuation and wavefield separation. 69th Ann. Internat. Mtg. Soc. Expl. Geophys., pp. 1204-1207, 1999.

[3] D. C. Henley, Coherent noise attenuation in the radial trace domain, Geophysics, Volume 68, Issue 4, pp. 1408-1416, July-August 2003.

[4] D. C. Henley, Effective noise attenuation and deconvolution in the radial trace domain, SEG Expanded Abstracts 23, p. 1969 , 2004.

[5] A. Guitton, Coherent noise attenuation using Inverse Problems and Prediction Error Filters: *SEP*- 105, 27-48, 2000.

[6] A. Guitton, Coherent noise attenuation: A synthetic and field example, Stanford Exploration Project, Report 108, April 29, 2001.

[7] T. Nemeth, Imaging and filtering by Least-Squares migration: Ph.D. thesis. The University of Utah, 1996.

[8] Mark S. Gockenbach and WilliamW. Symes, Coherent noise suppression in velocity inversion, SEG Annual International Meeting, 1999.

[9] A. Guitton, Multiple attenuation in complex geology with a pattern-based approach, Geophysics, Vol. 70, No. 4; p. V97–V107, (July-August 2005).

[10] Stewart, R.R. and Schieck, D.G., 1993.3-D F-K filtering, J. Seis. Expl., 2: 41-54.

[11] P. Bakker, Image structure analysis for seismic interpretation, Ph.D. dissertation, Delft University of Technology, 2002.

[12] OA Gaussian approach uses the Gradient Structure Tensor

[13] S. M. O'Malley and I. A. Kakadiaris, Towards Robust Structure-Based Enhancement and Horizon Picking in 3-D Seismic Data, Proceedings of the IEEE Conference on Computer Vision and Pattern Recognition – CVPR04, pp. 482-489, Washington DC, 2004.

[14] P. Bergé, Y. Pomeau, Ch. Vidal. "L'ordre dans le chaos" Hermann (Eds.) Paris, 1984.

[15] H. Poincaré, Mémoire sur les courbes définies par une équation différentielle. Journal de mathématiques pures et appliquées 3rd ser. 7, 375–422; 8, 251–296. Repr. OEuvres de Henri Poincaré 1, 3–84, 1881–1882.

[16] A. Martinet, Colloque CL: Hydrodynamique et Instabilité, Journal de Physique 37, Supplement, 1976.

[17] F. Takens, Detecting Strange Attractors in Turbulence, Lecture Notes in Math, vol. 898. Springer, New York, 1981.

[18] S. Bennett, History of control engineering 1930–1955. IEEE Control Engineering, Vol. 47. London: Peter Peregrinu, 1993.

[19] S. Boyd and L. O. Chua, Dynamical systems need not have spectrum. IEEE Trans. On Circuit and Syst., CAS-32: 968-69, 1985.

[20] N.H. Packard, J.P. Crutchfield, J.D. Farmer, and R.S. Shaw, Geometry from a time series. Physical Review Letters, 45:712, 1980.

[21] T. Sauer, J. Yorke, and M. Casdagli, Embedology, J. Stat. Phys. 65, 579, 1991.

[22] E. Otto, Chaos in Dynamical Systems, Cambridge University Press, Cambridge, 1993.

[23] T.S. Parker and L. O. Chua, Practical numerical algorithm for chaotic systems, New York, Springer-Berlag, 1981.

[24] H. D. I. Abarbanel, Analysis of Observed Chaotic Data, New York: Springer-Verlag, 1996.

[25] J. Holzfuss and G. Mayer-Kress. An approach to error estimation in the application of dimension algorithms. In G. Mayer-Kress, eds.*Dimensions and Entropies in Chaotic Systems*, pp. 114-122. Springer-Verlag, New-York , N.Y., 1986.

[26] P. Brodatz, Textures, A Photographic Album for Artist and Designers', Dover Publications, INC., Mineola, New York, 1966.

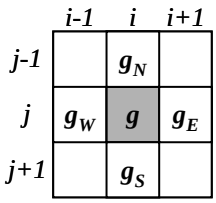

Figure 1

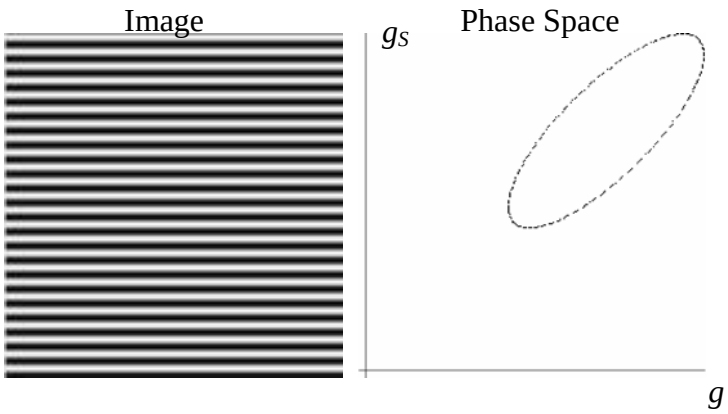

(*a*) (*b*)

Figure 2

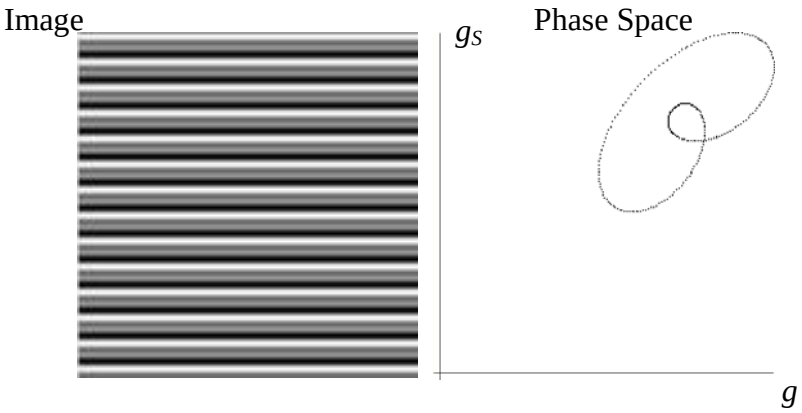

Figure 3

Image

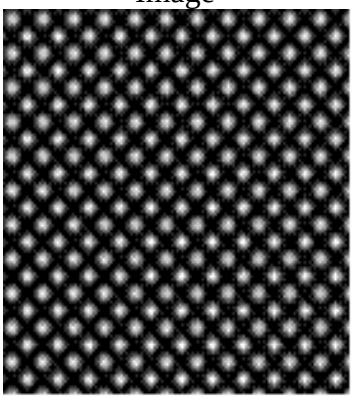

(*a*)

Phase space representations for different directional choices

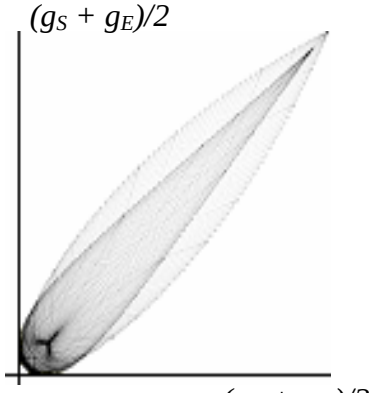

(*b*)

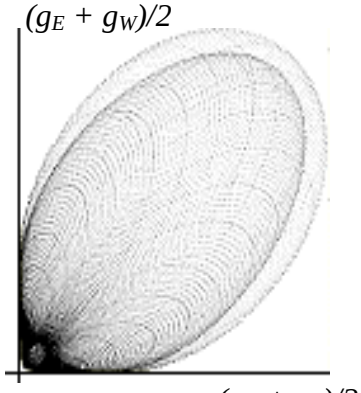

(*c*)

Figure 4

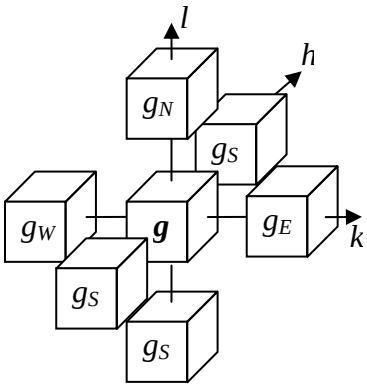

Figure 5

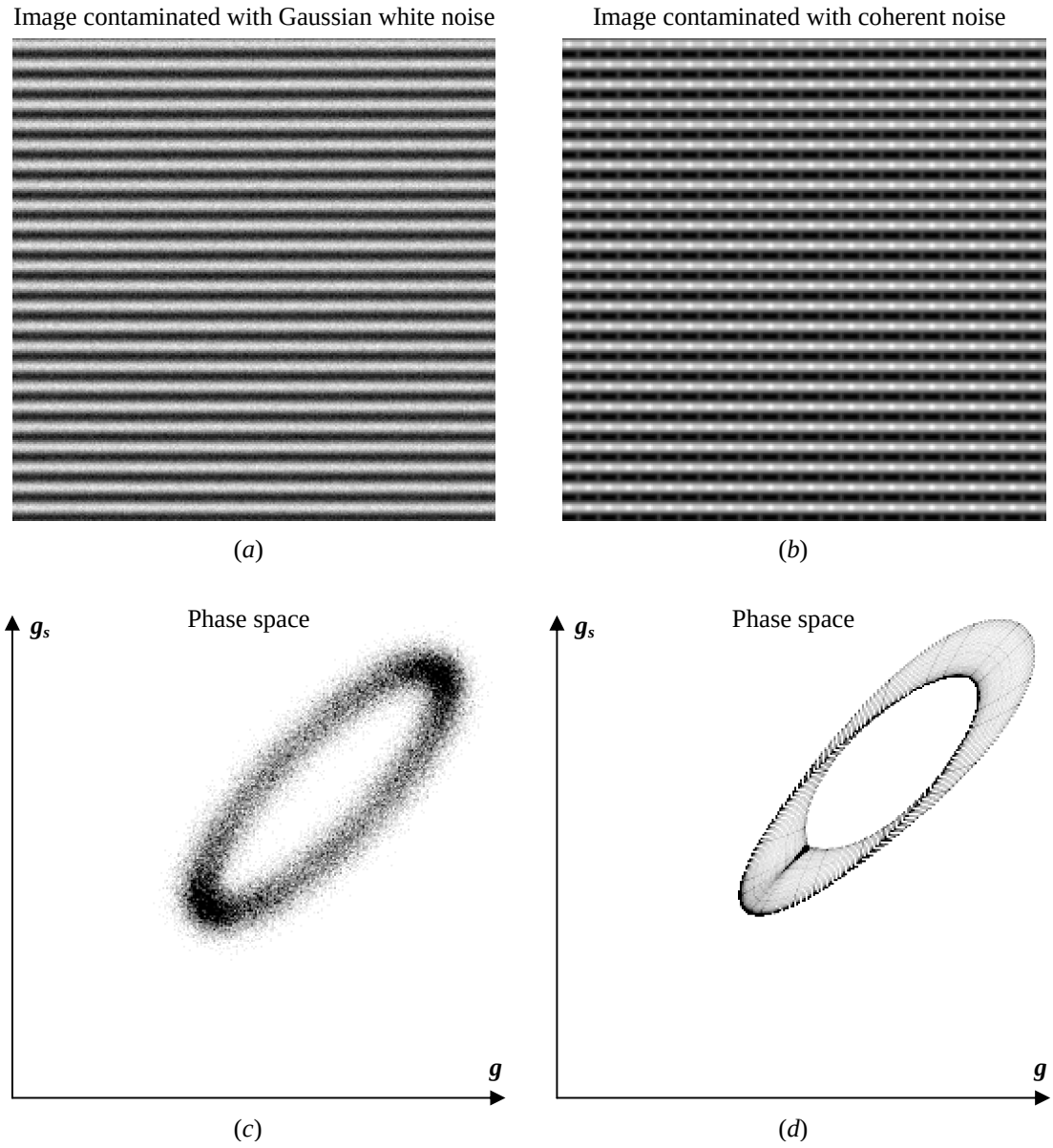
Image contaminated with Gaussian white noise
Image contaminated with coherent noise
(a)
(b)
Phase space
g_s
g
Phase space
g_s
g
(c)
(d)

Figure 6

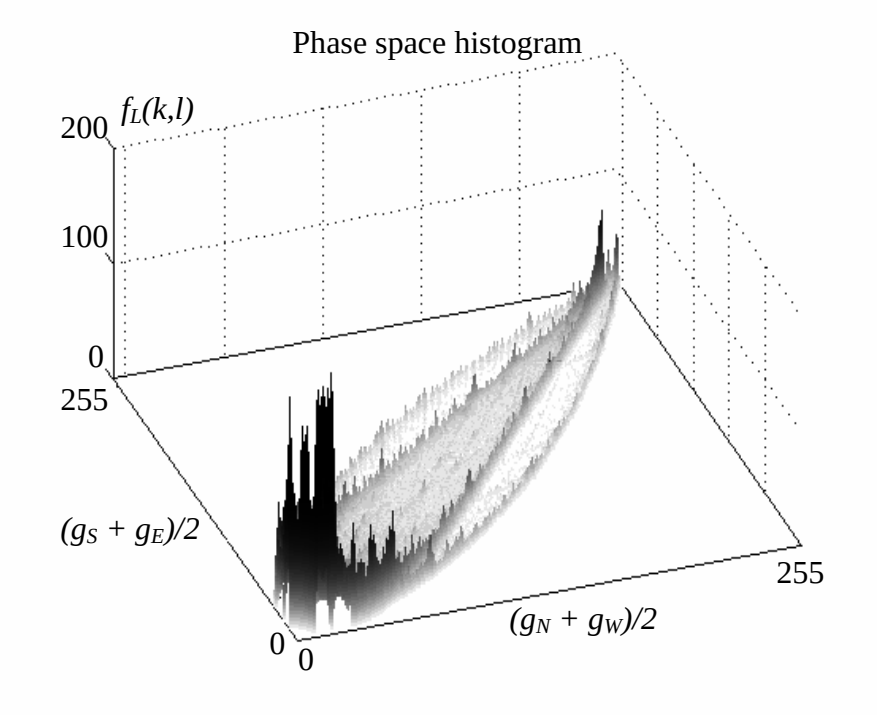

Figure 7

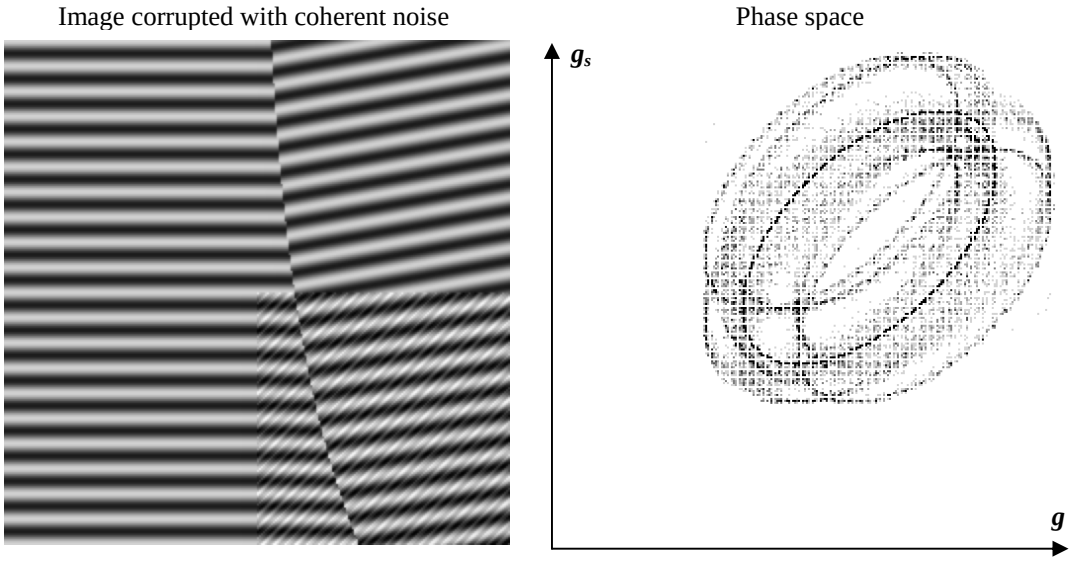

Figure 8

Tomographic section of composite fiber

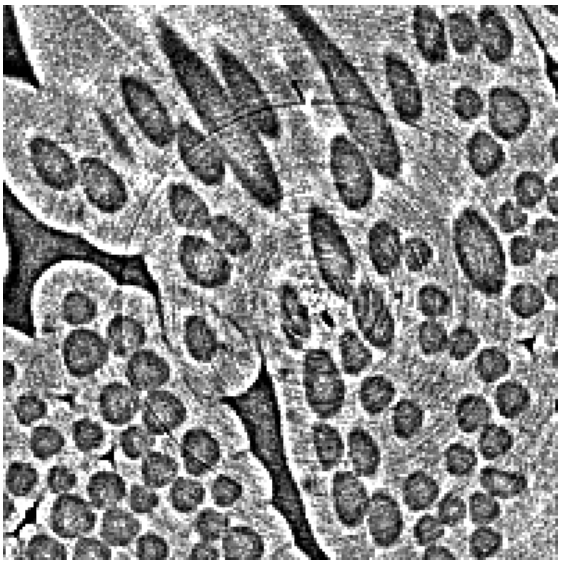

Figure 9

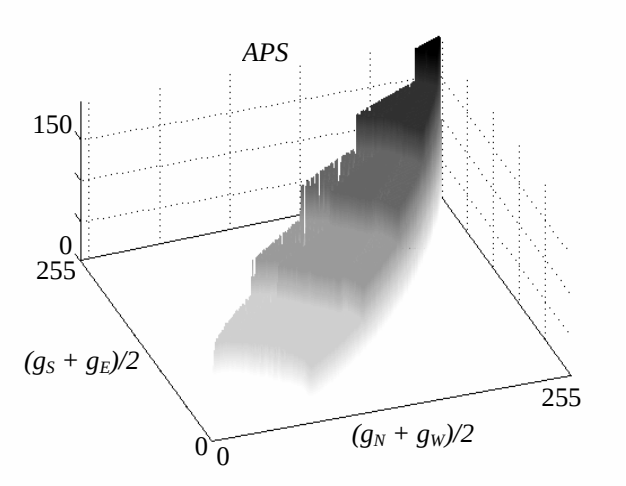

Figure 10

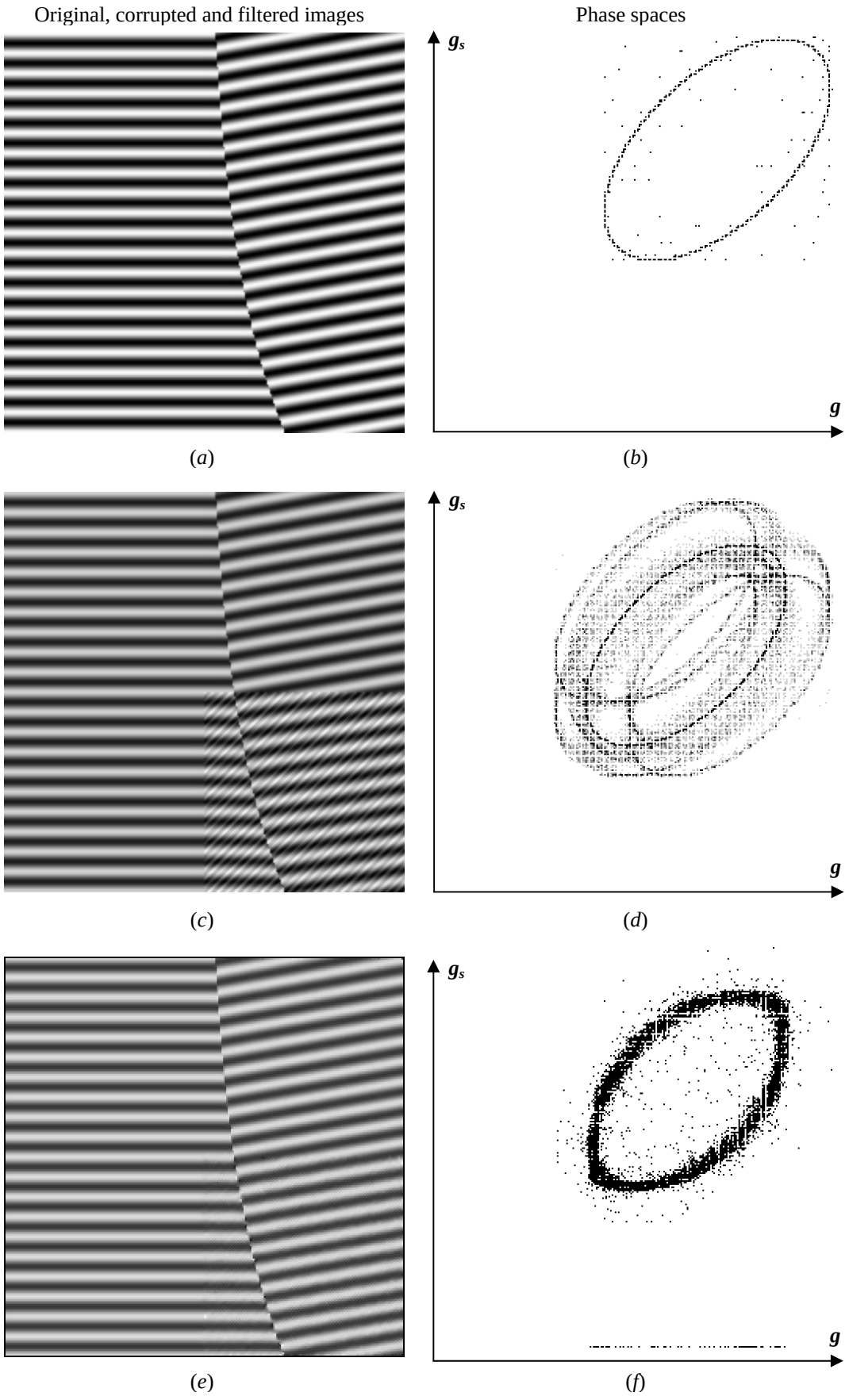
Original, corrupted and filtered images
Phase spaces
g_s
g
(a)
(b)
g_s
g
(c)
(d)
g_s
g
(e)
(f)

Figure 11

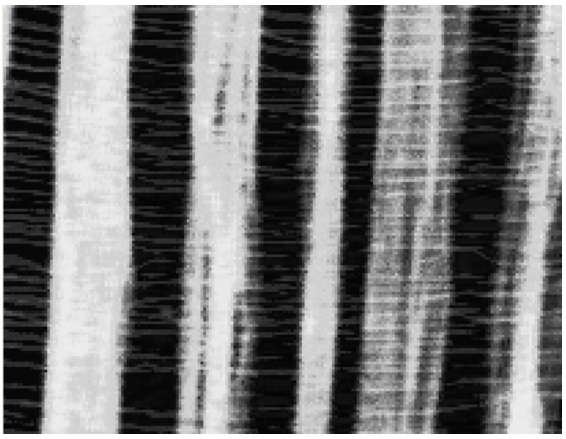

(*a*)

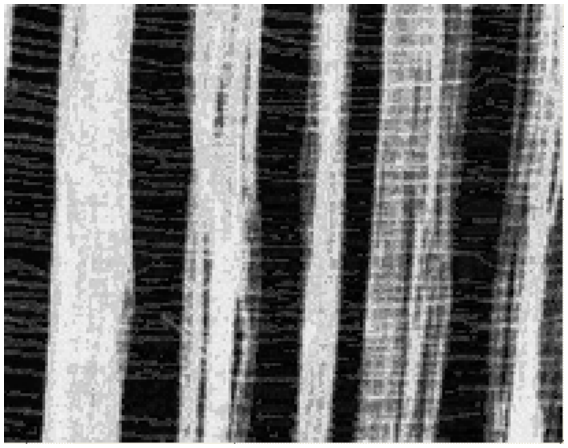

(*b*)

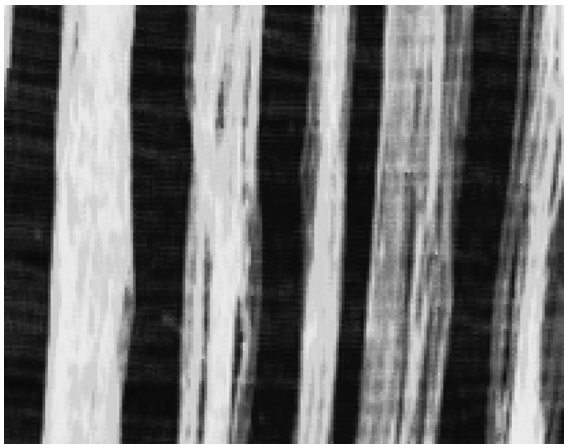

(*c*)

Figure 12

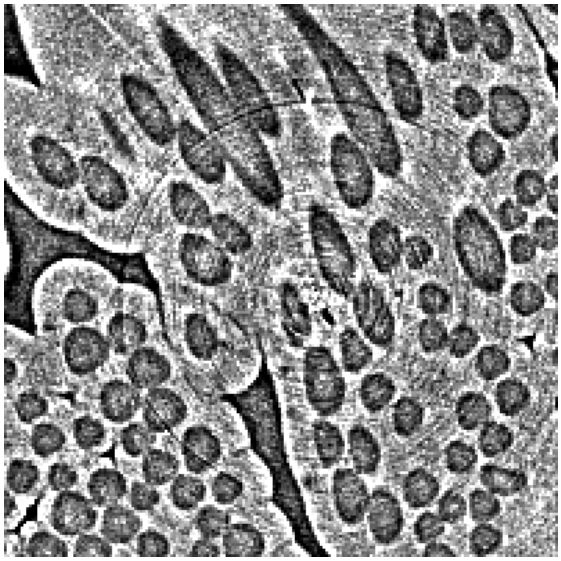

(*a*)

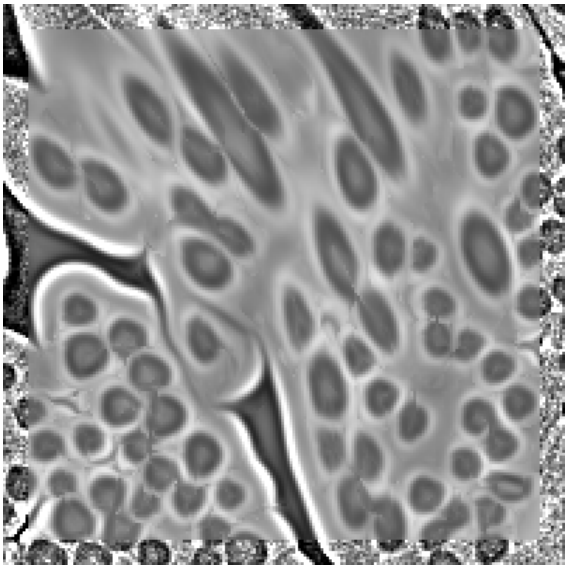

(*b*)

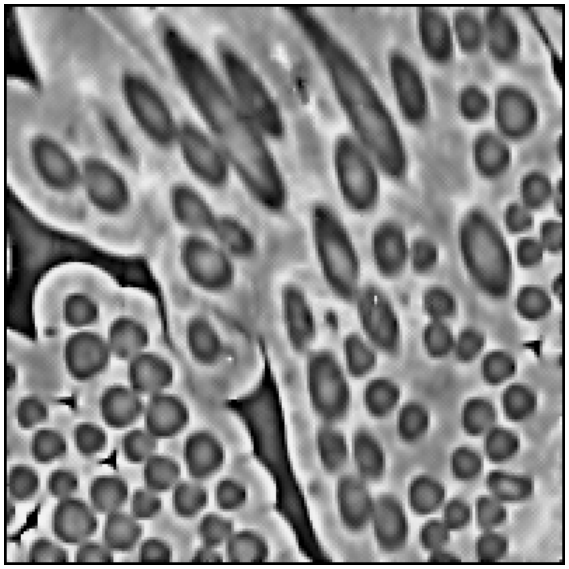

(*c*)

Figure 13

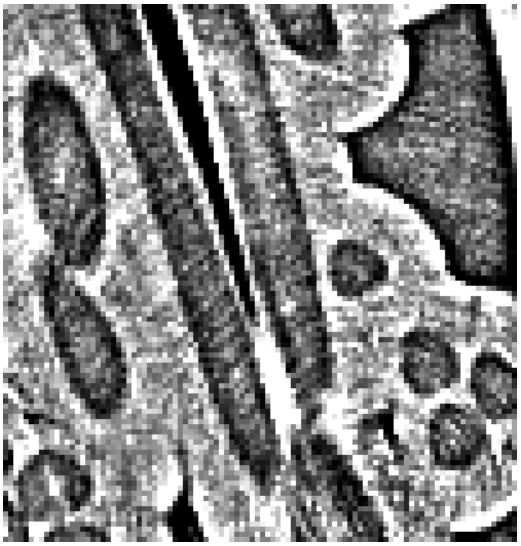

(*a*)

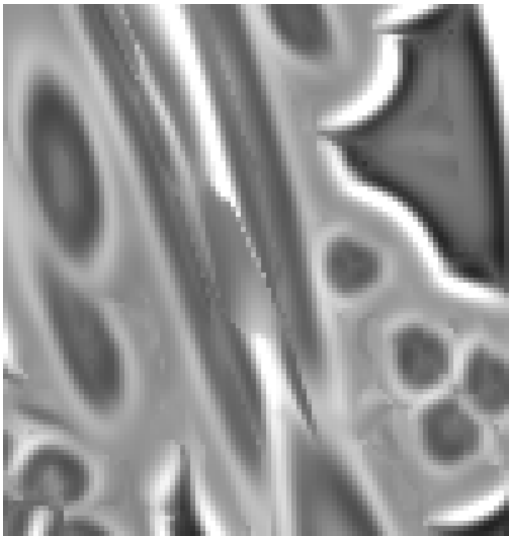

(*b*)

(*c*)

Figure 14